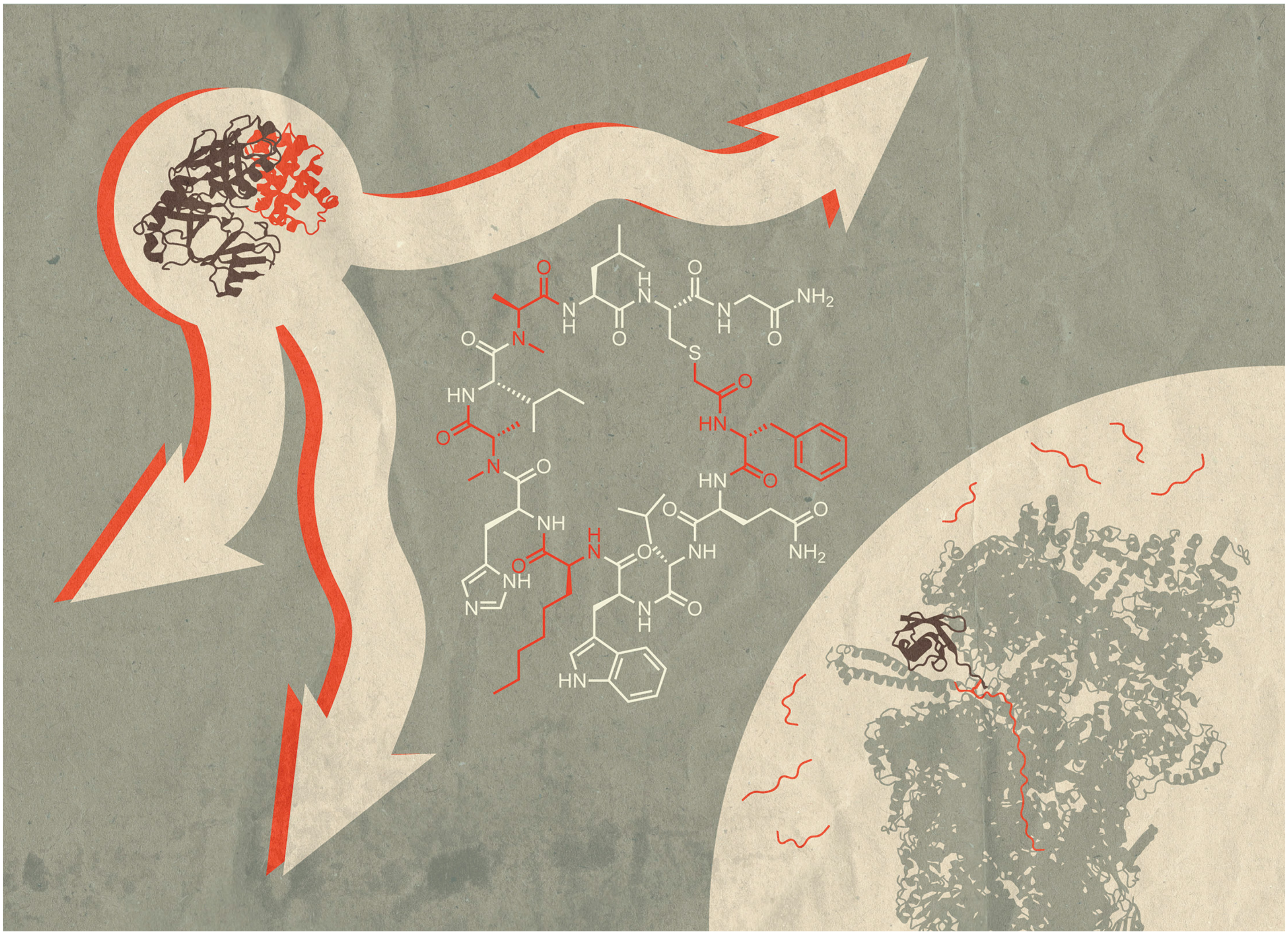

Showcasing research from Professor Ashraf Brik, Schulich Faculty of Chemistry, Technion-Israel Institute of Technology, Haifa, 3200008, Israel

In vivo modulation of ubiquitin chains by *N*-methylated non-proteinogenic cyclic peptides

The attachment of ubiquitin and ubiquitin chains are critical post-translational modifications. Diseases, like cancer, often involve dysregulation of this ubiquitin system. Here, we report the discovery of small, highly non-proteinogenic cyclic peptides which can tightly bind and modulate ubiquitin chains with particular Lys48-linkages. Our cyclic peptides block the action of deubiquitinases and the proteasome, induce apoptosis *in vitro,* and attenuate tumor growth *in vivo*. We conclude that modulating ubiquitin chains is a promising avenue for future anti-cancer therapeutics.

As featured in:

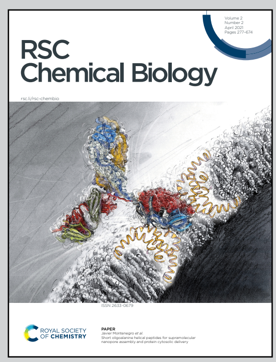

See Hiroaki Suga, Ashraf Brik *et al.*, *RSC Chem. Biol.*, 2021, **2**, 513.

RSC Chemical Biology

PAPER

View Article Online
View Journal | View Issue

Check for updates

Cite this: *RSC Chem. Biol.*, 2021, 2, 513

In vivo modulation of ubiquitin chains by *N*-methylated non-proteinogenic cyclic peptides†

Joseph M. Rogers, ‡[ab] Mickal Nawatha,‡[c] Betsegaw Lemma,[d] Ganga B. Vamisetti,[c] Ido Livneh,[e] Uri Barash,[e] Israel Vlodavsky,[e] Aaron Ciechanover,[e] David Fushman,[d] Hiroaki Suga *[a] and Ashraf Brik *[c]

Cancer and other disease states can change the landscape of proteins post-translationally tagged with ubiquitin (Ub) chains. Molecules capable of modulating the functions of Ub chains are potential therapeutic agents, but their discovery represents a significant challenge. Recently, it was shown that *de novo* cyclic peptides, selected from trillion-member random libraries, are capable of binding particular Ub chains. However, these peptides were overwhelmingly proteinogenic, so the prospect of *in vivo* activity was uncertain. Here, we report the discovery of small, non-proteinogenic cyclic peptides, rich in non-canonical features like *N*-methylation, which can tightly bind Lys48-linked Ub chains. These peptides engage three Lys48-linked Ub units simultaneously, block the action of deubiquitinases and the proteasome, induce apoptosis *in vitro*, and attenuate tumor growth *in vivo*. This highlights the potential of non-proteinogenic cyclic peptide screening to rapidly find *in vivo*-active leads, and the targeting of ubiquitin chains as a promising anti-cancer mechanism of action.

Received 3rd October 2020,
Accepted 30th November 2020

DOI: 10.1039/d0cb00179a

rsc.li/rsc-chembio

Introduction

Ubiquitination is an abundant post-translational modification.[1] Indeed, hundreds of enzymes exist to attach the small, 76 amino acid protein ubiquitin (Ub) mainly to lysine side-chains of particular cellular proteins.[2] Ub itself has multiple lysines, onto which further Ub can be attached. As a result, there are many possible Ub chains of various lengths and linkage types. These Ub chains can differently perturb the tagged protein[3,4] or be recognized by different cellular receptors, allowing them to perform different functions.[5,6] Lys48-linked Ub chains are particularly important, as these direct their tagged proteins for degradation by the 26S proteasome.[7]

Cancer cells use the ubiquitin–proteasome system to remove critical proteins and evade programmed cell death.[8] Consequently, inhibitors of the 26S proteasome have proved powerful research tools and successful anticancer therapeutics,[9] although resistance can emerge.[10] An attractive alternative is to target the signal for degradation: find molecules to bind to and interfere with the recognition of Lys48-linked Ub chains.[11–15] However, given the breadth of cellular processes that rely on differently linked Ub chains, specificity is crucial[5] and also a challenge due to the following reasons: Ub chains are assembled from the same monomer, and the differences in structure and dynamics of differently linked-Ub chains can be subtle.[16,17] Moreover, chain length is also important. For example, tetra Ub (Lys48-linked, $^{K48}Ub_4$) is postulated to be the minimal chain length to label a protein for degradation,[7] although there is some evidence suggesting shorter chains can also perform this function.[18,19] Molecules specific for long (*e.g.* ≥ 3), Lys48-linked Ub chains are required to specifically modulate protein degradation.

Ub chains have proved challenging targets for traditional drug discovery using small molecules. Those discovered to date suffer from weak binding and poor specificity for linkage and length.[12–15] Typically, these are symmetric molecules that bind monomeric Ub weakly, and then achieve what affinity they have for Ub chains through multimeric interactions. However, true recognition of Ub chains with a specific linkage was achieved recently using an alternative modality – *de novo* cyclic peptides.[11]

[a] Department of Chemistry, Graduate School of Science, The University of Tokyo, 7-3-1 Hongo, Bunkyo-ku, Tokyo 113-0033, Japan
E-mail: hsuga@chem.s.u-tokyo.ac.jp
[b] Department of Drug Design and Pharmacology, University of Copenhagen, Copenhagen 2100, Denmark
[c] Schulich Faculty of Chemistry, Technion-Israel Institute of Technology, Haifa 3200008, Israel. E-mail: abrik@technion.ac.il
[d] Department of Chemistry and Biochemistry, Center for Biomolecular Structure and Organization, University of Maryland, College Park, MD 20742, USA
[e] The Rappaport Faculty of Medicine and Research Institute, Technion-Israel Institute of Technology, Haifa 31096, Israel

† Electronic supplementary information (ESI) available: The data that support the findings of this study are available from the corresponding authors upon reasonable request. See DOI: 10.1039/d0cb00179a

‡ These authors contributed equally.

Nawatha *et al.* discovered *de novo* cyclic peptides capable of specifically binding Lys48-linked Ub chains. To achieve this, they first used solid-phase peptide synthesis (SPPS) coupled to Lys analogue native chemical ligation[20,21] to generate Lys48-linked Ub chains.[11] These Ub chains were of sufficient purity for use as targets for the RaPID system, a method that uses reprogrammed ribosome peptide synthesis to synthesize, and then screen, extremely large ($>10^{12}$) cyclic peptide libraries for binding molecules.[22] Tight-binding, having low nM K_D, and linkage-specific cyclic peptides were discovered, and their novel Ub recognition abilities were explained by their binding modes. The cyclic peptide bound in one orientation on the symmetric Ub chain target, simultaneously interacting with two or more Ub in the chains. Importantly, these cyclic peptides inhibited Ub chain recognition *in vitro* and had activity when added to cells, causing Ub-conjugate accumulation and apoptosis.[11]

Unfortunately, these first-generation cyclic peptides did not necessarily exhibit physicochemical properties comparable to known drug-like cyclic peptides. Orally-available, membrane-permeable, macrocyclic and cyclic peptides, such as the natural product cyclosporin, tend to be small ($\leq$1.2 kDa)[23,24] and have few H-bond acceptors, fewer H-bond donors, and no formal charges at pH 7.[25–27] Key to accessing this property space using peptides is the use of non-canonical amino acids, such as amine *N*-methylation,[28] which have the added benefit of conferring protease-resistance. By contrast, the first-generation Ub chain binding cyclic peptides were large ($\sim$1.7 kDa) and made almost entirely of H-bond-rich, protease-recognizable, canonical amino acids.[11]

A better subclass of cyclic peptides with improved bioactivity targeting the ubiquitin–proteasome system is needed to provide research tools and drug leads. A potential route to such molecules is to screen cyclic peptide libraries which include from the beginning non-canonical amino acids known to confer desirable physical properties.[22,29] However, it is not yet known if cyclic peptides from such a library can succeed at a challenging molecular recognition task like specific Ub chain binding. Here, we constructed and screened a highly non-proteinogenic peptide library to discover *de novo* cyclic peptides capable of modulating specific Lys48-linked ubiquitin chains.

Results

Target Ub chain synthesized by total chemical synthesis

To discover binders specific for the Lys48-linked Ub tetramer, while also avoiding binders that use di- or mono-Ub as the recognition element, high purity $^{K48}Ub_4$ and $^{K48}Ub_2$ chains were required. Ub chains were assembled by total chemical synthesis, as described previously,[11,20,21] for use as the target and anti-target respectively. Each was biotinylated at the N-terminus for attachment to a streptavidin solid support, enabling screening of pooled libraries of peptides.

Construction of a highly non-proteinogenic cyclic peptide library

We sought to create a large cyclic peptide library containing multiple non-canonical amino acids, to emulate the properties of drug-like, highly non-proteinogenic cyclic peptides. To form cyclic peptides, the genetic code was reprogrammed so that ribosomal peptide synthesis was initiated using a chloroacetyled amino acid.[30] We withdrew the natural initiator amino acid Met and its cognate aaRS during the construction of a custom reconstituted *in vitro* translation system,[31] and supplemented this with initiator tRNA loaded with ClAc-D-Phe,[22] using an artificial ribozyme flexizyme.[32] We then further reprogrammed the genetic code to remove the charged amino acids Glu, Asp, and Arg, and add the following non-canonical amino acids:[22,29,33] three *N*-methylated: MeGly, MeAla and MePhe; two D-stereochemistry: D-Phe and D-Ala, and the linear hydrophobic side-chain Aoc (Fig. 1A). Each was flexizyme-loaded onto tRNA and supplied to the translation system. The two D-amino acids were loaded onto an optimized $tRNA^{Pro}$ and the translation system supplemented with the *E. coli* translation factor EF-P to enhance translation efficiency.[34,35] To test the fidelity of this extensively reprogrammed 22 amino-acid genetic code (Fig. S1A, ESI†), we confirmed the ribosomal synthesis of peptides containing these non-canonical amino acids, with the major products detected by MALDI-TOF MS having the expected masses (Fig. S1B, ESI†).

Non-proteinogenic cyclic peptide library construction and selection

Following the RaPID protocol,[22] we assembled a greater than trillion-member cyclic peptide library using the ribosome and our reprogrammed genetic code, using degenerate DNA codons to encode cyclic peptides with 6–12 randomized amino acids each (Fig. 1B). mRNA display[36] was used to covalently tag each unique cyclic peptide with its encoding mRNA/DNA, for later resynthesis of the library, sequencing, or both. In the first round of screening, the cyclic peptide library was incubated with the target $^{K48}Ub_4$, the bound mRNA/DNA amplified and the enriched library resynthesized. Subsequent rounds included a ‘negative selection’ step where $^{K48}Ub_2$ and streptavidin binders were discarded before incubation with $^{K48}Ub_4$. This was to avoid a problem encountered in the first cyclic peptide screenings effort,[11] where the majority of the cyclic peptides recovered used $^{K48}Ub_2$ as the main recognition element, then using multimeric interaction to bind the longer chain target $^{K48}Ub_4$.

After each round, the fraction of mRNA/DNA recovered increased, suggesting an enrichment for desired $^{K48}Ub_4$-binding peptides (Fig. S2, ESI†). Next-generation sequencing (NGS) was then used to assess the library composition after each round of selection, and this showed the progressive enrichment of particular, putative $^{K48}Ub_4$-binding, peptide sequences (Fig. 1C). The top DNA sequence, and that of an analogue, were resubmitted to the *in vitro* translation system to confirm the integrity of the reprogrammed genetic code. The expected cyclic peptides, named **Ub4a** and **Ub4e** respectively (Fig. 1C), were detected by MALDI-TOF MS (Fig. S3, ESI†). **Ub4a** and **Ub4e** each contain an 11 amino acid macrocycle, with two *N*-methyl amino acids, a non-canonical side-chain as well as a D-amino acid. **Ub4e** contains a His, which may be partially

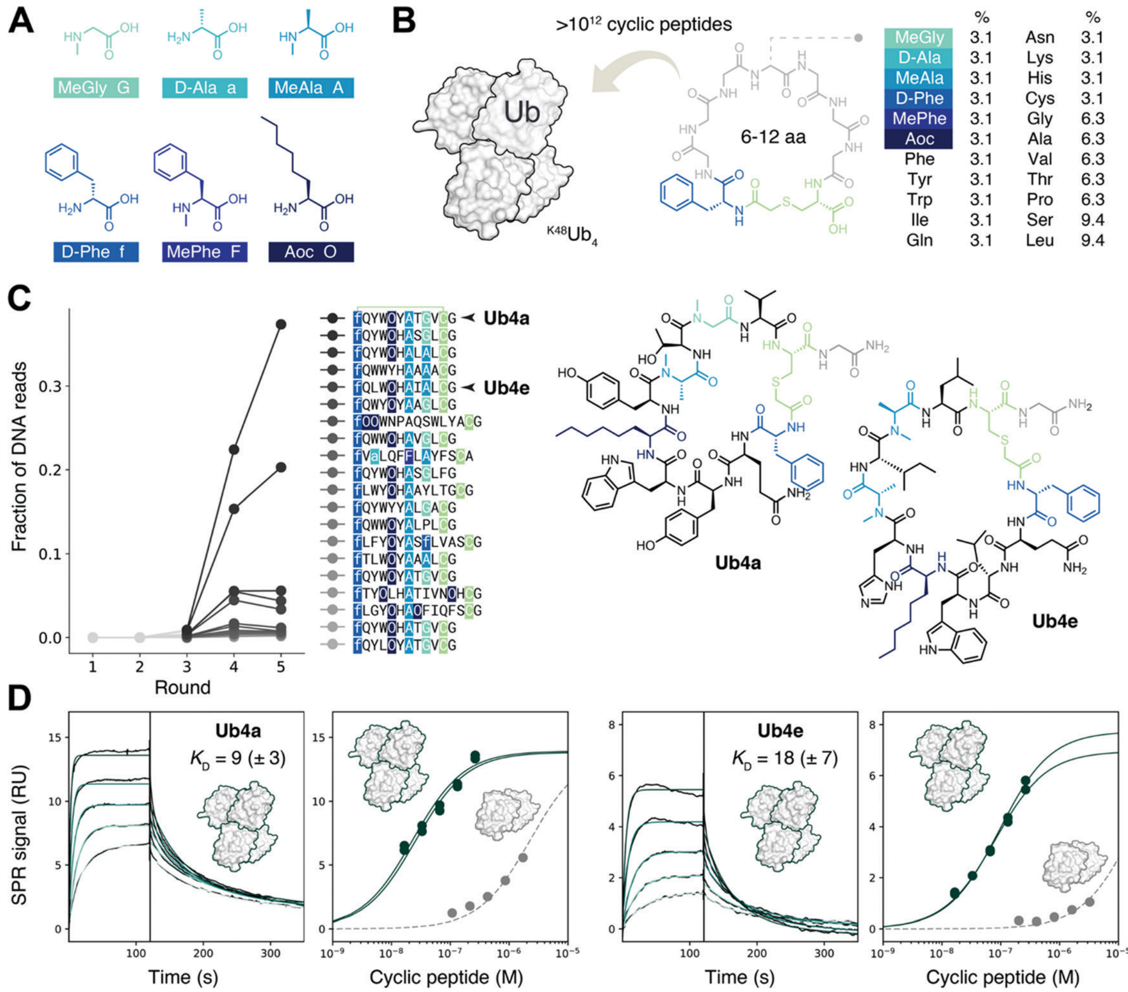

Fig. 1 Discovery of tight-binding non-proteinogenic cyclic peptides for the K48-linked ubiquitin tetramer. (A) The six non-canonical amino acids, replacing Met, Glu, Asp and Arg, used in the extensively reprogrammed genetic code used for cyclic peptide discovery. In addition, the initiation codon was reprogrammed to chloroacetyl-D-Phe which, after reaction with Cys, allows for the formation of cyclic peptides. (B) Amino acid distribution in the randomized sequence of the trillion-member cyclic peptide library screened against $^{K48}Ub_4$. (C) Cyclic peptide library composition, inferred from next generation sequencing of the DNA library, after five rounds of RaPID selection with $^{K48}Ub_4$ as the target and $^{K48}Ub_2$ as the anti-target. The library became enriched in certain cyclic peptide sequences, such as the highlighted **Ub4a** and **Ub4e**. (D) Surface plasmon resonance (SPR) kinetics (left) reveals tight (nM K_D) binding of cyclic peptide **Ub4a** to $^{K48}Ub_4$. Binding traces shown for 17, 33, 66, 130 and 260 nM cyclic peptide. SPR amplitudes upon titration (center left) suggests binding to $^{K48}Ub_2$ (grey) has a K_D in the μM range, significantly weaker binding than to $^{K48}Ub_4$ (data from two titrations shown, dark green). Similar selective binding observed for cyclic peptide **Ub4e** (centre right and right).

protonated at pH 7. Otherwise, as hoped, **Ub4a** and **Ub4e** are uncharged peptides with no formally charged amino acids at neutral pH.

Cyclic peptides preferentially bind longer K48-linked Ub chains

Cyclic peptides **Ub4a** and **Ub4e** were both synthesized by SPPS and tested for binding to the target $^{K48}Ub_4$ by SPR, and both displayed high affinity, nM K_D, for the Ub chain (Fig. 1D and Table S1, ESI†). As expected, binding to the anti-target $^{K48}Ub_2$ was considerably weaker, with >100 fold higher K_D, (Fig. 1D and Fig. S4 and Table S2, ESI†). To further confirm binding, we synthesized **Ub4a** labelled with a fluorescein dye (Fig. S5, ESI†) and used this as a probe for Ub-chains transferred onto nitrocellulose membranes (Fig. S6A and B, ESI†). Under these denaturing conditions, $^{K48}Ub_2$ and $^{K48}Ub_4$ bound **Ub4a**-fluorescein, with greater intensity then alternatively linked dimers $^{K63}Ub_2$ and $^{K11}Ub_2$.

NMR reveals unit- and residue-specific interactions between Ub chains and cyclic peptide Ub4a

We used NMR to confirm the physical interaction between cyclic peptide **Ub4a** and Ub chains as well as to map the Ub units and residues involved in binding. The unlabeled peptide was titrated into a solution of selectively ^{15}N-labeled Ub chains, and the binding was monitored by NMR. For this purpose, $^{K48}Ub_4$, $^{K48}Ub_3$, and $^{K48}Ub_2$ with specific Ub units uniformly ^{15}N-enriched were assembled from respective recombinant Ub monomers using controlled enzymatic chain assembly methodology.[11,37,38] The addition of **Ub4a** to $^{K48}Ub_4$ caused strong residue-specific perturbations in the ^1H–^{15}N NMR

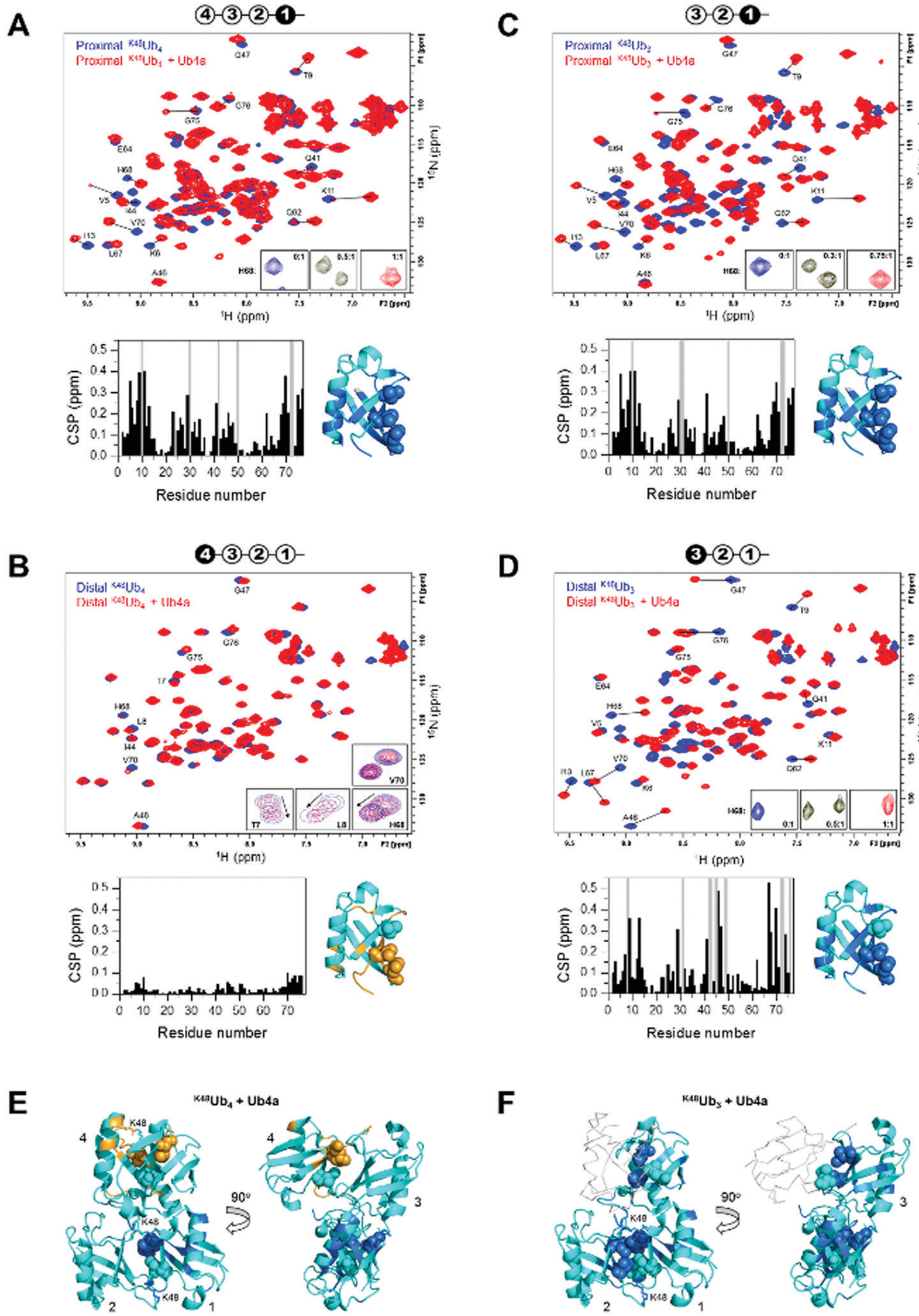

Fig. 2 Cyclic peptide **Ub4a** binds to hydrophobic patch residues in K48-linked tri- and tetra-Ub and engages first three Ub units in the chain. Shown are overlays of ^{1}H–^{15}N NMR spectra of free (blue) and **Ub4a**-bound (red) states of the proximal (A) and distal (B) Ub units of $^{K48}Ub_4$ and proximal (C) and distal (D) Ub units of $^{K48}Ub_3$. Select residues are indicated and their signals in the free and peptide-bound states are connected by lines. Insets in A, C, and D zoom on the signals of H68 to illustrate the slow-exchange behavior (the numbers indicate peptide/polyUb molar ratio). Insets in B are examples of signal behavior in the course of titration (up to 2 : 1 molar ratio) for the indicated residues: fast exchange for T7, L8, H68 and slow exchange for V70. Cartoon drawings on the top of each spectrum indicate which Ub unit in each chain is ^{15}N-labeled (colored black) and acts as the reporter; the numbering of Ub units starts from the proximal Ub. The plots below each spectrum show residue-specific chemical shift perturbations (CSPs) for each Ub unit; the grey bars correspond to residues for which unbound signals disappeared but the bound signals could not be unambiguously identified. Shown to the right of each plot is the structure of Ub monomer (PDB ID: 1UBQ) with residues exhibiting significant CSPs mapped, colored marine (light orange for the distal Ub of $^{K48}Ub_4$); the side-chains of the hydrophobic patch residues L8, I44, V70 are shown as spheres. The threshold for CSP-based mapping was set to 0.15 ppm for all Ub units studied here except for the distal Ub (unit 4) of $^{K48}Ub_4$ where it was 0.03 ppm. The distal Ub of $^{K48}Ub_4$ is colored differently to emphasize the markedly different level of NMR spectral perturbations. (E and F) Map of the residues that showed significant CSPs upon **Ub4a** binding to $^{K48}Ub_4$ (E) and $^{K48}Ub_3$ (F) on the cartoon representation of the structure of the compact state of $^{K48}Ub_4$ (PDB ID: 2O6V[39]). Only Ub units analyzed in this work are mapped; the CSP threshold and coloring are the same as in A–D. The Ub units as well as K48 side chains involved in the isopeptide linkages are indicated. In panel F, Ub unit 4 which is absent in $^{K48}Ub_3$ is shown as a light grey backbone trace, for comparison.

spectra of the proximal Ub unit (the one bearing free C terminus) (Fig. 2A). We observed a gradual decrease in intensity of the 'unbound' signals accompanied by the appearance and increase of new ('bound') signals at a different position in the spectrum, a textbook example of slow exchange, consistent with the slow dissociation rates (~1 per minute) detected by SPR (Table S1, ESI†). The perturbed residues are located primarily in and around the L8-I44-V70 hydrophobic patch on Ub surface, as well as the α-helix, and for most residues, the spectral changes saturated at about 1 : 1 peptide : $^{K48}Ub_4$ molar ratio. However, substantially weaker changes in the NMR spectra were observed for the distal Ub (the opposite end of the chain) of $^{K48}Ub_4$, where the signal shifts were substantially smaller. Furthermore, most residues exhibited gradual signal shifts characteristic for fast exchange on the NMR time scale. The noncovalent Ub–Ub interactions in K48-linked chains are sufficiently weak to allow fast interconversion between closed (possessing Ub–Ub interface) and open conformations.[38–40] Thus, it is possible that **Ub4a** binding disrupts the interactions between distal Ub and the rest of the Ub chain (Fig. 2B). These results indicate that interactions with the distal Ub in the tetramer do not significantly contribute to **Ub4a** binding and suggests that $^{K48}Ub_3$ is the actual peptide-binding element.

To test this hypothesis, we analyzed **Ub4a** binding to the proximal, middle (endo), and distal Ub units of $^{K48}Ub_3$. All three Ub units exhibited slow-exchange behavior upon **Ub4a** titration indicative of tight binding. The observed spectral changes in the proximal Ub of $^{K48}Ub_3$ were almost indistinguishable from those in the proximal Ub of $^{K48}Ub_4$ (Fig. 2C and Fig. S7, ESI†), pointing to strong similarity in the peptide's contacts with the proximal Ub in both chains. Also, the distal Ub of $^{K48}Ub_3$ exhibited strong NMR signal shifts (Fig. 2D), in stark contrast with the distal Ub of $^{K48}Ub_4$ (see also Fig. S8, ESI†). Similar strong NMR signal shifts were observed for the middle Ub of $^{K48}Ub_3$ (Fig. S9, ESI†). While the structure of $^{K48}Ub_3$:**Ub4a** complex awaits determination, these results indicate that all three Ub units in $^{K48}Ub_3$ are engaged in tight interactions with **Ub4a** (Fig. 2E and F).

To further verify **Ub4a** selectivity for Ub chains longer than the dimer, **Ub4a** peptide was titrated into $^{K48}Ub_2$ with ^{15}N-labeled proximal Ub. In stark contrast with the proximal Ub in $^{K48}Ub_4$ and $^{K48}Ub_3$, here we observed little or no signal shifts in the NMR spectra as well as strong signal broadening/disappearance for several residues located on the hydrophobic patch surface of Ub (Fig. S10, ESI†). This behavior is indicative of intermediate exchange on the NMR time scale, consistent with faster dissociation rates hence weaker binding to $^{K48}Ub_2$ detected by SPR (Fig. S4 and Table S2, ESI†).

To summarize, the NMR results corroborate tight **Ub4a** binding to K48-linked Ub chains of length ≥3 and revealed differential and residue-specific physical interactions between the peptide and various Ub units in these chains. The observed spectral perturbations generally map **Ub4a** binding sites to the hydrophobic patch surfaces of the Ub units involved. However, there are clear differences in the strength, direction, and exchange regime of these perturbations depending on the chain length and the position of the Ub unit within each chain. In particular, the strikingly weaker changes in NMR spectra observed for the distal Ub of $^{K48}Ub_4$ suggest that it is the trimer (or the first three Ub units in the tetramer) that is the **Ub4a** recognition element in K48-linked chains.

Cyclic peptides prevent recognition of Ub chains by specific proteases and the proteasome

We chose to investigate whether binding of the discovered cyclic peptides can prevent their recognition of Ub-chains by interacting proteins. For example, deubiquitinating enzymes (DUBs) recognize Ub-chains and cleave the connecting isopeptide bond. The DUB OTUB1 is specific for K48-linked Ub-chains[41] and can digest $^{K48}Ub_4$ to shorter chains and monomer *in vitro* (Fig. 3A). However, in the presence of equimolar **Ub4a**, $^{K48}Ub_4$ is protected from the activity of OTUB1 (Fig. 3A). This suggests that binding to the Ub chain by the cyclic peptide can interfere with recognition by the DUB, protecting against DUB cleavage. **Ub4a** also offers some protection to $^{K48}Ub_2$ from cleavage by OTUB1 (Fig. S11A, ESI†). However, the cyclic peptide was not able to protect $^{K11}Ub_2$ or $^{K63}Ub_2$ from cleavage by the K11 linkage-specific DUB Cezanne[42] and the linkage non-specific USP2, respectively (Fig. S11B and C, ESI†). Likely this is due to the specificity of these cyclic peptides binding to Ub-chains with the K48-linkage.

A critical Ub-chain interacting protein is the 26S proteasome, which recognizes K48-linked Ub-chains in order to degrade the tagged protein. It is possible that the cyclic peptides, by binding the Ub-chain, can inhibit this recognition and degradation. To test this, we added synthetic α-globin-$^{K48}Ub_4$[43] to purified 26S proteasome *in vitro*, with and without **Ub4a** or **Ub4e**. Similar to the addition of the direct proteasome inhibitor MG132,[44] the cyclic peptides were able to protect α-globin-$^{K48}Ub_4$[43] from degradation by the 26S proteasome (Fig. 3B). Presumably, these cyclic peptides bind K48-linked Ub chains in a manner that prevents recognition by the 26S proteasome (Fig. 3B).

The NMR finding that only first three Ub units (counting from the proximal end) in $^{K48}Ub_4$ bind **Ub4a** tightly, was independently verified by comparing the ability of the peptide to protect $^{K48}Ub_4$ and $^{K48}Ub_3$ against disassembly by OTUB1 that preferentially cleaves from the distal end of a poly-Ub chain. The results (Fig. S12A, ESI†) show that **Ub4a** effectively shields $^{K48}Ub_3$ from disassembly by OTUB1, consistent with the NMR data showing tight peptide binding to all Ub units in the trimer. Interestingly, in the presence of **Ub4a**, OTUB1 cleaves only one Ub molecule from $^{K48}Ub_4$ resulting in visible and sustained accumulation of a trimer, thus supporting the conclusion that the distal Ub unit in the tetramer binds **Ub4a** loosely. A slightly different trend was observed for **Ub4a** protection against proteasome-associated DUB Ubp6, where some amount of $^{K48}Ub_4$ was reduced to a trimer but a significant portion of it remained unaffected (Fig. S12B, ESI†), likely reflecting Ubp6's preference for cleaving the *endo* isopeptide bond (between two middle Ubs) in $^{K48}Ub_4$.[45] By contrast,

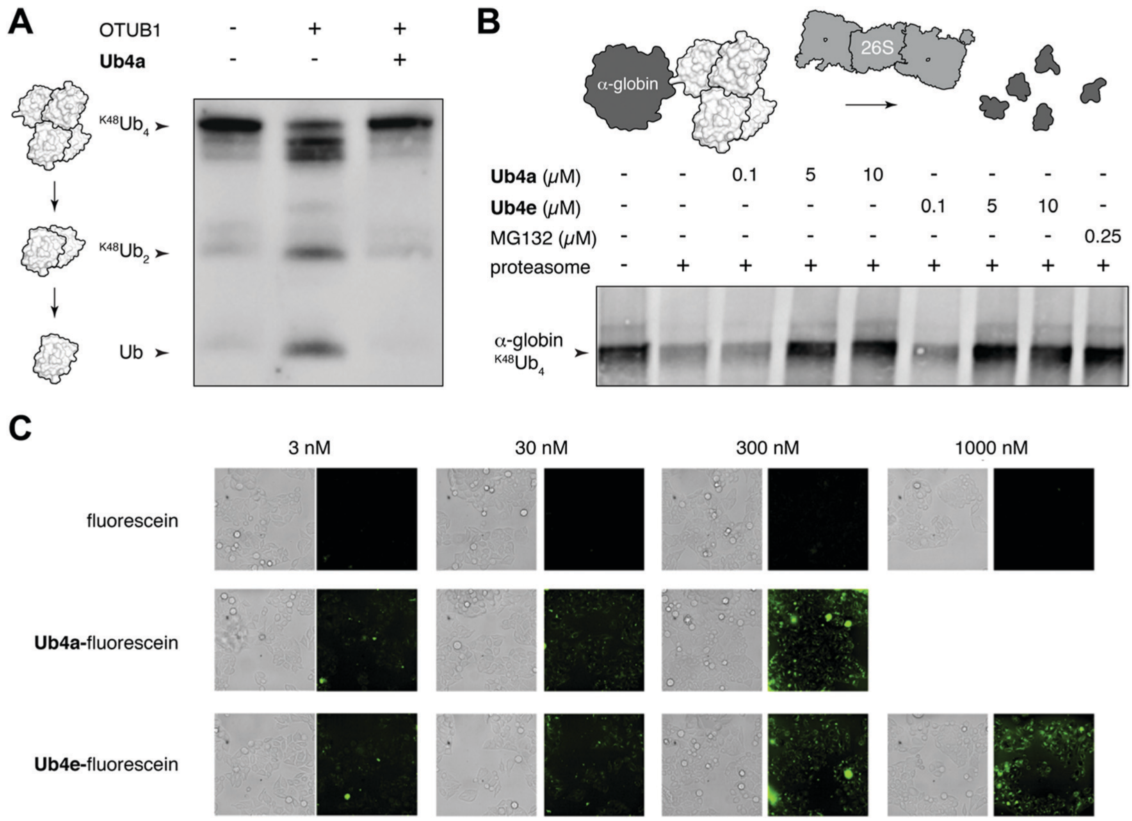

Fig. 3 Cyclic peptides inhibit Ub-dependent proteolysis and can enter cells. (A) Cyclic peptide **Ub4a** (2 μM) inhibits the cleavage of $^{K48}Ub_4$ (2 μM) by the K48-specific DUB OTUB1 (0.25 μM) *in vitro*. Western blot with anti-Ub antibody. (B) Cyclic peptides **Ub4a** and **Ub4e** inhibit degradation of $^{K48}Ub_4$-tagged HA-tagged α-globin (5 μM) by the 26S proteasome (150 nM) *in vitro*. Similar inhibition of degradation is observed in the presence of direct proteasome inhibitor MG132. Western blot with anti-HA antibody. (C) Cyclic peptides **Ub4a** and **Ub4e**, fluorescein labelled, are internalized by live HeLa cells.

Ub4a effectively blocked $^{K48}Ub_4$ disassembly by a general linkage-nonspecific DUB USP2 (Fig. S12C, ESI†).

Cyclic peptides can enter cells

Having shown that cyclic peptides can modulate the function of Ub-chains *in vitro*, we next sought to test their effects in live cells. However, as the ubiquitin system is largely intracellular, it was important to check their ability to enter these cells. We used fluorescein-labelled cyclic peptides (Fig. S5, ESI†) and live-cell imaging to monitor their entrance into HeLa cells. Uptake of **Ub4a**-fluorescein and **Ub4e**-fluorescein peptides could be observed after incubation for 2 hours with 3 nM peptide, whereas fluorescein alone showed negligible uptake even at 1000 nM (Fig. 3C). To quantify the uptake, we incubated HeLa cells with **Ub4a**-fluorescein for 16 h, the cells were washed and the residual fluorescence indicates significant retention of peptide-fluorescein relative to fluorescein alone (Fig. S13, ESI†).

Cyclic peptides lead to Ub-conjugates accumulation

We have shown using purified proteins that cyclic peptide binding can inhibit Ub-chain cleavage by DUB activity, and therefore might be expected to cause an accumulation of Ub-chains and proteins tagged with Ub-chains in the cell. We incubated HeLa cells with cyclic peptides **Ub4a** or **Ub4e**, as well as MG132, lysed the cells, separated the proteins and stained using anti-Ub western blot to detect Ub-conjugates. In a dose-dependent manner, the cyclic peptides **Ub4a** and **Ub4e** caused accumulation of intracellular Ub-conjugates, producing a similar effect to the proteasome inhibitor MG132 (Fig. 4A). Incidentally, cyclic peptide **Ub4a** could be used to detect these Ub-conjugates on the western blot membrane (Fig. S6C and D, ESI†).

Ub4a can induce apoptosis in cancer cell lines

Inhibition of the ubiquitin system using direct proteasome inhibitors can induce apoptosis, enabling these inhibitors to be used as cancer therapeutics.[46] We wanted to examine whether our cyclic peptides, through their Ub-chain binding, could also induce apoptosis.[47,48] We incubated **Ub4a** with the cancer-derived U87 cells, which are a human primary glioblastoma cell line (brain cancer), and cells sorted for their ability to bind fluorescently labelled annexin-V using Fluorescence Activated Cell Sorting (FACS), detecting both early and late apoptotic cells. **Ub4a** at 100 nM exhibited a clear increase in apoptosis after 24 h treatment, similar to the direct proteasome inhibitors: bortezomib, ixazomib, and carfilzomib[46] (Fig. 4B). Furthermore, we tested the effects of the cyclic peptides on three other cancer cell lines, SH-SY5Y cells (neuroblastoma), MDA-MB-231 cells (epithelial human breast cancer) and HeLa

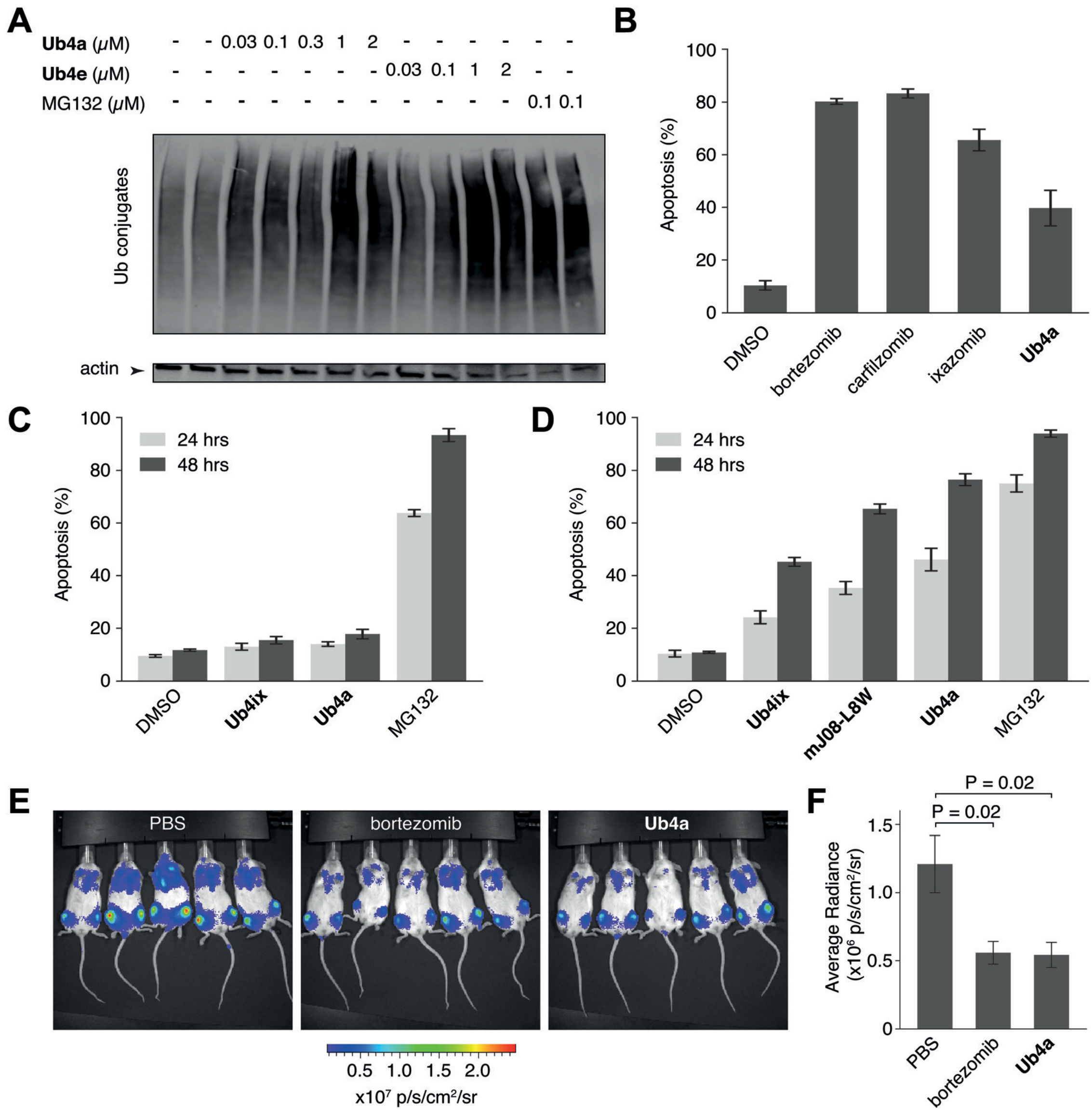

Fig. 4 Cyclic peptides cause intracellular accumulation of Ub-conjugates, induce apoptosis *in vitro* and show anti-cancer activity *in vivo*. (A) Addition of cyclic peptides **Ub4a** or **Ub4e** induced the accumulation of Ub-conjugates in live cells, in a dose-dependent manner. A similar effect was seen upon addition of the direct proteasome inhibitor MG132. (B) **Ub4a** (100 nM), induced apoptosis in the U87 cell line (brain cancer cell line, primary glioblastoma) after 24 h incubation. Apoptotic cells were detected using fluorescently labelled annexin-V and FACS. A similar induction of apoptosis was seen upon addition of (100 nM) direct proteasome inhibitors bortezomib, carfilzomib and ixazomib. (C) HEK-293 non-cancer derived (embryonic kidney) cells were exposed to the cyclic peptides **Ub4a**, **Ub4ix** or MG132 (10 μM), only MG132 showed significant induction of apoptosis. (D) Cyclic peptide **Ub4a** induces more apoptosis in U87 cells than previous generation Ub-binding peptides **Ub4ix** or **mJ08-L8W**, approaching the potency of direct proteasome inhibitor MG132 (all compounds at 100 nM). (E) Imaging of luciferase-expressing human CAG myeloma cells in mice shows that treatment with either the approved anti-cancer drug bortezomib, or the cyclic peptide **Ub4a**, inhibit the growth of tumors *in vivo*. (F) Quantification of luminescence from human tumor cells in mice shows that 15 days of treatment with **Ub4a** causes a reduction in tumor growth similar to treatment with bortezomib.

cells (cervical cancer) which all showed similar induction of apoptosis upon treatment with cyclic peptides (Fig. S14, ESI†). Interestingly, under these conditions the **Ub4a** cyclic peptide did not induce apoptosis in the HEK-293 cell line (embryonic kidney derived), whereas treatment with the direct proteasome inhibitor MG132 did induce apoptosis (Fig. 4C).

Finally, we compared the apoptotic induction abilities of the non-proteinogenic cyclic peptide **Ub4a** with two Ub-binding largely proteinogenic cyclic peptides from previous studies **Ub4ix**[11] and **mJ08-L8W**.[49] **Ub4a** was able to induce apoptosis in a greater proportion of U87 (Fig. 4D), SH-SY5Y, MDA-MB-231 and HeLa cells (Fig. S14, ESI†). One possible reason for the efficacy of **Ub4a** is that it is resistant to proteases. We tested the stability of **Ub4a** in human plasma and found that the non-proteinogenic cyclic peptide is very stable in human plasma, with a half-life of multiple days (~60 h) (Fig. S15, ESI†).

Ub4a shows anti-cancer activity *in vivo*

The plasma stability of **Ub4a** combined with its ability to induce apoptosis *in vitro* in cancer cells, led us to investigate if this *de novo* cyclic peptide might show anti-cancer activity *in vivo*. We sought to investigate whether **Ub4a** could inhibit the growth of human tumors in mice.[50] Briefly, SCID/NOD mice were injected intravenously with luciferase-expressing human CAG myeloma cells,[51] and after a week of growth, **Ub4a** (1 mg kg^{-1} twice a week) or the approved anti-cancer medication bortezomib[52] (0.5 mg kg^{-1} twice a week) were injected intraperitoneally. Both **Ub4a** and bortezomib treated mice showed a marked reduction in tumor progression relative to untreated mice (Fig. 4E, F and Fig. S16, ESI†). Even in this first test of *in vivo* activity, 15 days of **Ub4a** treatment resulted in a reduction in tumor growth similar to the bortezomib positive control (Fig. 4E and F).

Discussion

Ubiquitin chains are attractive targets for therapeutic intervention, given their central role in cellular activities and their frequent dysregulation in pathology.[53] Here, we report the discovery of non-proteinogenic cyclic peptides able to specifically bind and modulate long (>3) K48-linked Ub chains: the tag for protein degradation by the proteasome. In contrast to previous efforts,[11] the cyclic peptide library was built to include amino acids known to confer drug-like properties onto peptides, with the aim of generating Ub chain modulating molecules which are proteolytically stable and able to engage their intracellular target *in vivo*.

Using the RaPID system methodology, a cyclic peptide library was constructed to include D-stereocenteres, *N*-methylated backbones, non-canonical side chains, while being depleted in canonical charged amino acids, This library was screened against $^{K48}Ub_4$, and two hit non-proteinogenic *de novo* cyclic peptides were chosen for characterization in detail: **Ub4a** and **Ub4e**. Both tightly bound $^{K48}Ub_4$, and showed significantly weaker binding for shorter chain $^{K48}Ub_2$. NMR studies revealed that **Ub4a** uses $^{K48}Ub_3$ as the main recognition element. Interestingly, while $^{K48}Ub_4$ contains two overlapping $^{K48}Ub_3$ units, 1–3 and 2–4, it is specifically the proximal trimer, 1–3, that engages the cyclic peptide. Chemical shift perturbations upon binding map the binding interactions to residues in and around the surface hydrophobic patch on the Ub units involved (Fig. 2E and F). Overlaying these CSPs on the "closed" $^{K48}Ub_4$ structure, which is the predominant conformation in the apo form, suggests that cyclic peptide binding involves intercalation into the Ub–Ub interface. The binding mode of **Ub4a** is broadly similar to that of **Ub4ix**, a cyclic peptide from the previous study, which also used the proximal $^{K48}Ub_3$.[11] However, given the dissimilar chemical structures of **Ub4a** and **Ub4ix** (Fig. S17, ESI†), their interfaces with $^{K48}Ub_3$ are likely very different and await further characterization.

Natural product bioactive cyclic peptides are often highly non-proteinogenic: they are rich in non-canonical amino acids which confer protease resistance and passive membrane permeability. Moreover, these peptides tend to be small (<1000 Da), and lack amino acids that are charged at neutral pH. An archetype for this class is the orally available immunosuppressant cyclosporin.[33] Previously characterized Ub chain binding cyclic peptides, like **Ub4ix**, were quite unlike cyclosporin: they were highly proteinogenic, larger and rich in charged amino acids at neutral pH (Fig. S17, ESI†). Promisingly, the cyclic peptides characterized here, **Ub4a** and **Ub4e**, are highly non-proteinogenic, containing two *N*-methyl, a D-stereochemistry and a non-canonical aliphatic side-chain amino acid. They are small, with just 11-amino acids in the macrocycle, making them undecamer cyclic peptides similar to cyclosporin. Lastly, similar to cyclosporin, these peptides lack formal charges, having zero, or close to zero net charge in the case of **Ub4e**, at neutral pH (Fig. S17, ESI†).

Importantly, the physicochemical make-up of the peptide library, the non-canonical amino acids added and the charged canonical amino acids removed, did not preclude the discovery of cyclic peptides with impressive binding strength and specificity for the challenging $^{K48}Ub_4$ target. Indeed, the non-canonical rich cyclic peptides described here have similar binding affinities to previously discovered, largely canonical, cyclic peptides.[11] Yet the former have smaller macrocycles and had appreciably lower molecular mass, suggesting that the non-canonical amino acid collection is in fact superior at producing high-affinity, selective cyclic peptides.

We showed that **Ub4a** binding to Lys48-chain Ub chains prevents their recognition by deubiquitinates and the proteasome. Moreover, **Ub4a** can induce apoptosis in cancer cell lines *in vitro*, and attenuate the growth of tumor cells *in vivo*. These anti-cancer effects are likely due to disruption of Ub chain recognition processes which are part of the ubiquitin–proteasome system. Cancer cells are particularly dependent on the proteasome activity to remove certain proteins and evade programmed cell death, and this is the rationalization behind the anti-cancer effects observed for direct proteasome inhibitors such as bortezomib, carfilzomib, and ixazomib, which have been approved for the treatment of multiple myeloma.[54] Indeed, throughout our *in vitro* and *in vivo* trials, **Ub4a** and direct proteasome inhibitors show broadly similar effects and comparable efficacy, the latter is striking considering **Ub4a** is a hit from a screen and the proteasome inhibitors are the product of extensive optimization.

While **Ub4a** showed similar effects to the direct proteasome inhibitors, it is important to emphasize that these cyclic peptides act through a different mechanism, targeting a different component of the ubiquitin–proteasome system. Ub-chain binders might therefore overcome the shortcomings of current proteasome inhibitors, the acquired resistance and adverse side-effects which decrease patients' quality of life.[55,56] Non-proteinogenic cyclic peptide targeting of Ub chains, therefore, have great potential for the development of new anti-cancer therapeutics.

Author contributions

J. M. R. designed and performed the cyclic peptide discovery, carried out SPR assays, analysed the data, and co-wrote the manuscript and the ESI.† M. N. assisted in the chemical synthesis of cyclic peptides, carried out *in vitro* and cellular assays and co-wrote the manuscript and the ESI.† B. L. synthesized isotope-labelled Ub chains, conducted the NMR studies and assisted with writing the paper. G. B. V. assisted in the synthesis of cyclic peptides. I. L. carried out the confocal microscopy assay and assisted with cellular studies. U. B. carried out the *in vivo* assays and I. V. assisted in the design of the *in vivo* assays. A. C. assisted in the design of the confocal microscopy assay and *in vitro* and cellular studies. D. F. designed and supervised the NMR studies, carried out data analysis and assisted with writing the manuscript and the ESI.† Hi. S. supervised the RaPID study and assisted in the writing of the paper. A. B. designed and supervised the entire project and the writing of the paper.

Data availability

The data that support the findings of this study are available from the corresponding authors upon reasonable request.

Conflicts of interest

There are no conflicts to declare.

Acknowledgements

A. B. holds the Jordan and Irene Tark Academic Chair. This project has received funding from the European Research Council (ERC) under the European Union's Horizon 2020 research and innovation program (grant agreement no. [831783]). This work was also supported by Japan Agency for Medical Research and Development (AMED), Platform Project for Supporting Drug Discovery and Life Science Research (Basis for Supporting Innovative Drug Discovery and Life Science Research) under JP20am0101090 to H. S. J. M. R. was supported by Grants-in-aid for JSPS Fellows (P13766), a joint ANR-JST grant (ANR-14-JITC-2014-003 and JST-SICORP) and the Novo Nordisk Foundation (0054441).

References

1 A. Hershko and A. Ciechanover, *Annu. Rev. Biochem.*, 1998, **67**, 425–479.
2 C. E. Berndsen and C. Wolberger, *Nat. Struct. Mol. Biol.*, 2014, **21**, 301–307.
3 D. Morimoto, E. Walinda, H. Fukada, K. Sugase and M. Shirakawa, *Sci. Rep.*, 2016, **6**, 39453.
4 T. Hagai and Y. Levy, *Proc. Natl. Acad. Sci. U. S. A.*, 2010, **107**, 2001–2006.
5 D. Komander and M. Rape, *Annu. Rev. Biochem.*, 2012, **81**, 203–229.
6 R. Yau and M. Rape, *Nat. Cell Biol.*, 2016, **18**, 579–586.
7 J. S. Thrower, L. Hoffman, M. Rechsteiner and C. M. Pickart, *EMBO J.*, 2000, **19**, 94–102.
8 J. Adams, *Cancer Cell*, 2004, **5**, 417–421.
9 X. Huang and V. M. Dixit, *Cell Res.*, 2016, **26**, 484–498.
10 S. Lu and J. Wang, *Biomark Res.*, 2013, **1**, 13.
11 M. Nawatha, J. M. Rogers, S. M. Bonn, I. Livneh, B. Lemma, S. M. Mali, G. B. Vamisetti, H. Sun, B. Bercovich, Y. Huang, A. Ciechanover, D. Fushman, H. Suga and A. Brik, *Nat. Chem.*, 2019, **11**, 644–652.
12 T. Nguyen, M. Ho, K. Kim, S. I. Yun, P. Mizar, J. W. Easton, S. S. Lee and K. K. Kim, *Molecules*, 2019, **24**, 1073.
13 T. Nguyen, M. Ho, A. Ghosh, T. Kim, S. I. Yun, S. S. Lee and K. K. Kim, *Biochem. Biophys. Res. Commun.*, 2016, **479**, 33–39.
14 M. A. Nakasone, T. A. Lewis, O. Walker, A. Thakur, W. Mansour, C. A. Castaneda, J. L. Goeckeler-Fried, F. Parlati, T. F. Chou, O. Hayat, D. Zhang, C. M. Camara, S. M. Bonn, U. K. Nowicka, S. Krueger, M. H. Glickman, J. L. Brodsky, R. J. Deshaies and D. Fushman, *Structure*, 2017, **25**(1839–1855), e1811.
15 R. Verma, N. R. Peters, M. D'Onofrio, G. P. Tochtrop, K. M. Sakamoto, R. Varadan, M. Zhang, P. Coffino, D. Fushman, R. J. Deshaies and R. W. King, *Science*, 2004, **306**, 117–120.
16 Y. Ye, G. Blaser, M. H. Horrocks, M. J. Ruedas-Rama, S. Ibrahim, A. A. Zhukov, A. Orte, D. Klenerman, S. E. Jackson and D. Komander, *Nature*, 2012, **492**, 266–270.
17 C. A. Castaneda, A. Chaturvedi, C. M. Camara, J. E. Curtis, S. Krueger and D. Fushman, *Phys. Chem. Chem. Phys.*, 2016, **18**, 5771–5788.
18 Y. Lu, B. H. Lee, R. W. King, D. Finley and M. W. Kirschner, *Science*, 2015, **348**, 1250834.
19 I. Livneh, Y. Kravtsova-Ivantsiv, O. Braten, Y. T. Kwon and A. Ciechanover, *BioEssays*, 2017, **39**, 1700027.
20 K. S. Ajish Kumar, M. Haj-Yahya, D. Olschewski, H. A. Lashuel and A. Brik, *Angew. Chem., Int. Ed.*, 2009, **48**, 8090–8094.
21 S. N. Bavikar, L. Spasser, M. Haj-Yahya, S. V. Karthikeyan, T. Moyal, K. S. Kumar and A. Brik, *Angew. Chem., Int. Ed.*, 2012, **51**, 758–763.
22 Y. Yamagishi, I. Shoji, S. Miyagawa, T. Kawakami, T. Katoh, Y. Goto and H. Suga, *Chem. Biol.*, 2011, **18**, 1562–1570.
23 C. R. Pye, W. M. Hewitt, J. Schwochert, T. D. Haddad, C. E. Townsend, L. Etienne, Y. Lao, C. Limberakis, A. Furukawa, A. M. Mathiowetz, D. A. Price, S. Liras and R. S. Lokey, *J. Med. Chem.*, 2017, **60**, 1665–1672.
24 P. Matsson and J. Kihlberg, *J. Med. Chem.*, 2017, **60**, 1662–1664.
25 B. C. Doak, B. Over, F. Giordanetto and J. Kihlberg, *Chem. Biol.*, 2014, **21**, 1115–1142.
26 B. Over, P. Matsson, C. Tyrchan, P. Artursson, B. C. Doak, M. A. Foley, C. Hilgendorf, S. E. Johnston, M. D. T. Lee, R. J. Lewis, P. McCarren, G. Muncipinto, U. Norinder, M. W. Perry, J. R. Duvall and J. Kihlberg, *Nat. Chem. Biol.*, 2016, **12**, 1065–1074.
27 M. R. Naylor, A. T. Bockus, M. J. Blanco and R. S. Lokey, *Curr. Opin. Chem. Biol.*, 2017, **38**, 141–147.
28 J. Chatterjee, F. Rechenmacher and H. Kessler, *Angew. Chem., Int. Ed.*, 2013, **52**, 254–269.
29 T. Passioura, W. Liu, D. Dunkelmann, T. Higuchi and H. Suga, *J. Am. Chem. Soc.*, 2018, **140**, 11551–11555.
30 Y. Goto, A. Ohta, Y. Sako, Y. Yamagishi, H. Murakami and H. Suga, *ACS Chem. Biol.*, 2008, **3**, 120–129.

31 Y. Shimizu, A. Inoue, Y. Tomari, T. Suzuki, T. Yokogawa, K. Nishikawa and T. Ueda, *Nat. Biotechnol.*, 2001, **19**, 751–755.
32 Y. Goto, T. Katoh and H. Suga, *Nat. Protoc.*, 2011, **6**, 779–790.
33 C. L. Ahlbach, K. W. Lexa, A. T. Bockus, V. Chen, P. Crews, M. P. Jacobson and R. S. Lokey, *Future Med. Chem.*, 2015, **7**, 2121–2130.
34 T. Katoh, Y. Iwane and H. Suga, *Nucleic Acids Res.*, 2017, **45**, 12601–12610.
35 T. Katoh, I. Wohlgemuth, M. Nagano, M. V. Rodnina and H. Suga, *Nat. Commun.*, 2016, **7**, 11657.
36 R. W. Roberts and J. W. Szostak, *Proc. Natl. Acad. Sci. U. S. A.*, 1997, **94**, 12297–12302.
37 V. Ranjani, M. Assfalg and D. Fushman, *Methods Enzymol.*, 2005, **399**, 177–192.
38 R. Varadan, O. Walker, C. Pickart and D. Fushman, *J. Mol. Biol.*, 2002, **324**, 637–647.
39 M. J. Eddins, R. Varadan, D. Fushman, C. M. Pickart and C. Wolberger, *J. Mol. Biol.*, 2007, **367**, 204–211.
40 Y. E. Ryabov and D. Fushman, *J. Am. Chem. Soc.*, 2007, **129**, 3315–3327.
41 T. E. Mevissen, M. K. Hospenthal, P. P. Geurink, P. R. Elliott, M. Akutsu, N. Arnaudo, R. Ekkebus, Y. Kulathu, T. Wauer, F. El Oualid, S. M. Freund, H. Ovaa and D. Komander, *Cell*, 2013, **154**, 169–184.
42 A. Bremm, S. M. Freund and D. Komander, *Nat. Struct. Mol. Biol.*, 2010, **17**, 939–947.
43 H. Sun, S. M. Mali, S. K. Singh, R. Meledin, A. Brik, Y. T. Kwon, Y. Kravtsova-Ivantsiv, B. Bercovich and A. Ciechanover, *Proc. Natl. Acad. Sci. U. S. A.*, 2019, **116**, 7805–7812.
44 A. L. Goldberg, *J. Cell Biol.*, 2012, **199**, 583–588.
45 W. Mansour, M. A. Nakasone, M. von Delbruck, Z. Yu, D. Krutauz, N. Reis, O. Kleifeld, T. Sommer, D. Fushman and M. H. Glickman, *J. Biol. Chem.*, 2015, **290**, 4688–4704.
46 R. J. Deshaies, *BMC Biol.*, 2014, **12**, 94.
47 L. J. Crawford, B. Walker and A. E. Irvine, *J. Cell Commun. Signaling*, 2011, **5**, 101–110.
48 E. E. Manasanch and R. Z. Orlowski, *Nat. Rev. Clin. Oncol.*, 2017, **14**, 417–433.
49 Y. Huang, M. Nawatha, I. Livneh, J. M. Rogers, H. Sun, S. K. Singh, A. Ciechanover, A. Brik and H. Suga, *Chemistry*, 2020, **26**, 8022–8027.
50 U. Barash, M. Lapidot, Y. Zohar, C. Loomis, A. Moreira, S. Feld, C. Goparaju, H. Yang, E. Hammond, G. Zhang, J. P. Li, N. Ilan, A. Nagler, H. I. Pass and I. Vlodavsky, *J. Natl. Cancer Inst.*, 2018, **110**, 1102–1114.
51 M. Weissmann, G. Arvatz, N. Horowitz, S. Feld, I. Naroditsky, Y. Zhang, M. Ng, E. Hammond, E. Nevo, I. Vlodavsky and N. Ilan, *Proc. Natl. Acad. Sci. U. S. A.*, 2016, **113**, 704–709.
52 J. Adams, V. J. Palombella, E. A. Sausville, J. Johnson, A. Destree, D. D. Lazarus, J. Maas, C. S. Pien, S. Prakash and P. J. Elliott, *Cancer Res.*, 1999, **59**, 2615–2622.
53 D. Vilchez, I. Saez and A. Dillin, *Nat. Commun.*, 2014, **5**, 5659.
54 L. D. Fricker, *Annu. Rev. Pharmacol. Toxicol.*, 2020, **60**, 457–476.
55 G. S. Kaplan, C. C. Torcun, T. Grune, N. K. Ozer and B. Karademir, *Free Radical Biol. Med.*, 2017, **103**, 1–13.
56 F. S. Liu, *Taiwan. J. Obstet. Gynecol.*, 2009, **48**, 239–244.